

# Second-Order Nonlinear Optical Activity Induced by Ordered Dipolar Chromophores Confined in the Pores of an Anionic Metal–Organic Framework\*\*

Jiancan Yu, Yuanjing Cui,\* Chuande Wu, Yu Yang, Zhiyu Wang, Michael O’Keeffe, Banglin Chen,\* and Guodong Qian\*

Organic second-order nonlinear optical (NLO) materials have potential applications in high-speed electro-optic modulators and all-optical data processing devices. Thus these materials have attracted considerable attention over the past decade.<sup>[1,2]</sup> Among the prerequisites such as large chromophore hyperpolarizability ( $\beta$ ), chromophore number density, and efficient acentric molecular ordering, efficient ordering is the most crucial while most challenging task for achieving large bulk second-order NLO responses. Although a variety of organic chromophores with high  $\beta$  values have been developed for a long time, so far no powerful strategy has been realized to induce efficient acentric molecular ordering, and thus the use of these organic chromophores as nonlinear optical materials is limited. The developed strategies for inducing noncentrosymmetric arrangements of dipolar chromophores which include electric-field poling and self-assembly suffer from intermolecular dipole–dipole interactions among the packed chromophores.<sup>[3–7]</sup>

To make use of the pore confinement effect of the emerging porous metal–organic frameworks (MOFs)<sup>[8–23]</sup> for specific inclusion of guest substrates, a few microporous MOFs have been targeted for the efficient polymerization and separation of xylene isomers.<sup>[24–26]</sup> In principle, it should

also be possible to encapsulate matching ordered dipolar chromophores in the pores of a porous MOFs; however, this has never been realized. Herein we report the first example of a microporous MOF that includes the ordered organic dipolar chromophore 4-(4-(diphenylamino)styryl)-1-dodecylpyridinium bromide (DPASD) and forms a highly NLO active anionic MOF (ZJU-28 $\supset$ DPASD; ZJU = Zhejiang University).

Reaction of 4,4',4''-benzene-1,3,5-triyl-tribenzoic acid ( $H_3$ BTB) and  $InCl_3$  in *N,N*-dimethylformamide/1,4-dioxane/ $H_2O$  at 130 °C affords the colorless needle-like crystals of  $(Me_2NH_2)_3[In_3(BTB)_4] \cdot 12DMF \cdot 22H_2O$  (ZJU-28). Compound ZJU-28 crystallizes in the  $P\bar{6}2c$  space group, which has a symmetric element, *c*, and thus does not show a second-order nonlinear optical response. In the crystal structure of ZJU-28, the eight-coordinated indium centers act as nodes, which are connected by two  $H_3$ BTB linkers parallel to the *ab* plane and another two linkers roughly perpendicular to *ab* plane. Therefore, every indium center is coordinated by four  $H_3$ BTB linkers and can be seen as a four-fold connected node, and every tritropic  $H_3$ BTB linker is a three-fold connected node (Figure 1a). The underlying net of ZJU-28 is an unusual MOF and, we believe, not described before. The net is quite different from the default net expected for tetrahedral and planar triangular vertices.<sup>[27]</sup> The net is remarkably self-entangled and it has for a net composed of low-coordinated vertices a high density. The net is made up of three families of parallel corrugated  $6^3$  nets that are interwoven so that a layer of each family is catenated to all the members of the other two families as shown in Figure 1b. Two periodic  $6^3$  nets are joined by further links to make the whole structure just one (3,4)-coordinated net to which the RCSR (recticular chemistry structure resource) symbol jcy has been assigned.<sup>[28]</sup>

Two types of 1D channels along a *c* axis of about  $6.1 \times 6.1$  and  $7.1 \times 8.5 \text{ \AA}^2$  exist, respectively. The channels and void spaces were occupied by abundant highly disordered solvent and cationic  $Me_2NH_2$  molecules, which were estimated to be 64.7% of the total volume.

Encouraged by the fact that the cationic  $Me_2NH_2$  molecules can be readily exchanged by metal cations such as  $Cu^{2+}$ ,  $Ni^{2+}$ , and  $Eu^{3+}$ , we examined the potential of ZJU-28 to encapsulate different pyridinium hemicyanine chromophores (Figure 2a) to develop nonlinear optical MOF materials. To our surprise, four different pyridinium hemicyanine cationic chromophores with a systematically changed alkyl chain length, 4-(4-(diphenylamino)styryl)-1-methylpyridi-

[\*] J. C. Yu, Prof. Dr. Y. J. Cui, Dr. Y. Yang, Prof. Dr. Z. Y. Wang, Prof. Dr. B. Chen, Prof. Dr. G. D. Qian  
State Key Laboratory of Silicon Materials  
Cyrus Tang Center for Sensor Materials and Applications  
Department of Materials Science and Engineering  
Zhejiang University, Hangzhou, 310027 (China)  
E-mail: cuiyj@zju.edu.cn  
gdqian@zju.edu.cn

Prof. Dr. C. D. Wu  
Department of Chemistry, Zhejiang University  
Hangzhou, 310027 (China)

Prof. Dr. M. O’Keeffe  
Department of Chemistry and Biochemistry  
Arizona State University, Tempe, AZ 85287 (USA)

Prof. Dr. B. Chen  
Department of Chemistry, University of Texas at San Antonio  
San Antonio, TX 78249 (USA)  
E-mail: banglin.chen@utsa.edu

[\*\*] This work was supported by the National Natural Science Foundation of China (grant numbers 50928201, 50972127, and 51010002) and the Fundamental Research Funds for the Central Universities, and partially supported by the Welch Foundation (grant number AX-1730, B.C.).

Supporting information for this article is available on the WWW under <http://dx.doi.org/10.1002/anie.201204160>.

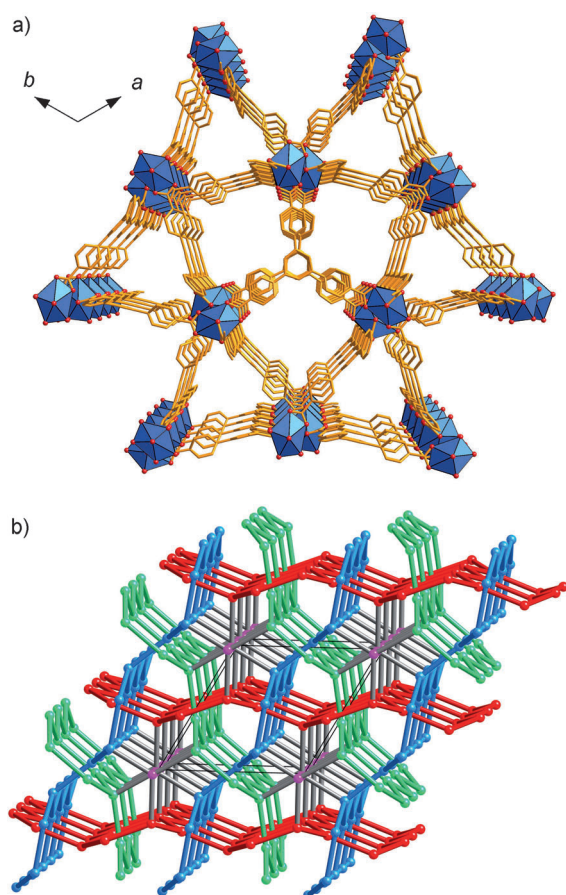


**Figure 1.** a) Crystal structure of ZJU-28 viewed along the crystallographic *c* direction, (In, blue polyhedra; C, orange; O, red; H atoms,  $\text{Me}_2\text{NH}_2^+$  ions, and solvent molecules are omitted for clarity. b) The underlying net of ZJU-28. Three interwoven families of  $6^3$  nets, shown in green, blue, and red, are linked by further three-coordinated vertices (magenta) to form a continuous three-periodic jcy net.

nium (DPASM), 1-butyl-4-(4-(diphenylamino)styryl)pyridinium (DPASB), 4-(4-(diphenylamino)styryl)-1-nonylpyridinium (DPASN), and 4-(4-(diphenylamino)styryl)-1-dodecylpyridinium (DPASD) can be easily incorporated into the corresponding framework materials by immersing the as-synthesized ZJU-28 in DMF, which contains different hemicyanine chromophores, for eight days at  $60^\circ\text{C}$  to give ZJU-28 $\supset$ DPASM, ZJU-28 $\supset$ DPASB, ZJU-28 $\supset$ DPASN, and ZJU-28 $\supset$ DPASD with a chromophore content of 27.6, 28.2, 29.8, and 22.9 wt %, respectively. These new hemicyanine chromophore-including MOF materials have been characterized by FTIR and luminescent spectroscopies and fluorescent microscopy. Compared with the as-synthesized ZJU-28 which displays after excitation at 365 nm an emission of blue light at 414 nm, the new MOF material ZJU-28 $\supset$ DPASD shows a red emission peak at 634 nm (Figure 2b and Figure S6 in the Supporting Information). This unique feature makes it possible to visualize the distribution of the cationic chromophores simply by fluorescent microscopy.

A laser confocal scanning microscope was used to follow the distribution of cationic chromophores within the host MOF materials. After the as-synthesized ZJU-28 crystals

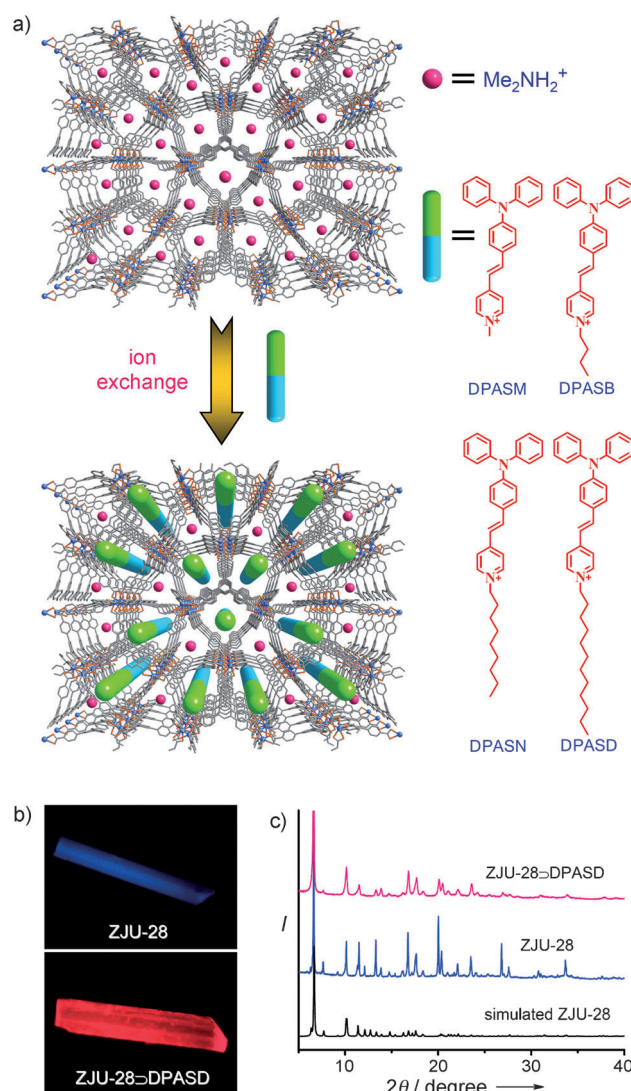


**Figure 2.** a) Schematic illustration of pyridinium hemicyanine chromophores incorporated into ZJU-28; b) Fluorescent microscope images of ZJU-28 and ZJU-28 $\supset$ DPASD illuminated with light of 365 nm UV; c) PXRD patterns of ZJU-28 and ZJU-28 $\supset$ DPASD.

were for several hours immersed in the DMF solution containing the dye molecules, a bright-red emission was observed from the end regions of the crystals. The luminescent emissive regions gradually spread over the whole MOF crystal once the immersion time has been increased to several days. As shown in Figure S7 in the Supporting Information, all slices of various depths show the same fluorescent image profile and three selected regions in the crystal show the same luminescent spectra, indicating that the hemicyanine chromophore DPASD ions have been uniformly distributed within ZJU-28 $\supset$ DPASD. ZJU-28 $\supset$ DPASD is a highly crystalline material which retains the original crystal structure of ZJU-28, as shown by the powder X-ray diffraction (PXRD) patterns (Figure 2c).

To study nonlinear optical properties, second harmonic generation (SHG) measurements were performed on these hemicyanine chromophore-including ZJU-28 materials by the

Kurtz powder technique using a Q-switched Nd:YAG pulse laser with a 1064 nm as fundamental frequency laser.<sup>[29]</sup> The output signals were collected by a fiber spectrometer at 520 to 560 nm, to distinguish the SHG signals from fluorescence emission. As shown in Figure 3a,c, the inclusion of these hemicyanine chromophores tunes the ZJU-28 MOF material

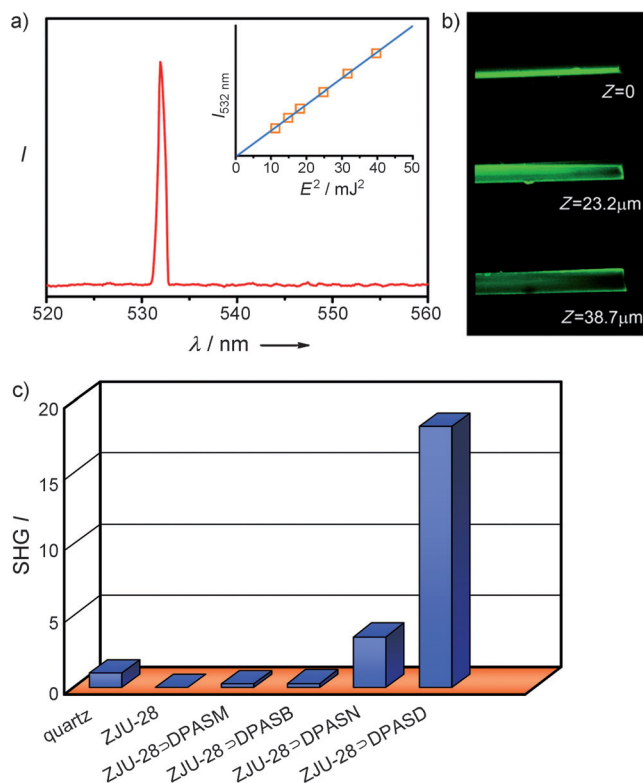


**Figure 3.** a) SHG spectra of ZJU-28 DPASD. Inset: The SHG intensity of ZJU-28 DPASD as a function of the energy of the fundamental frequency laser. b) Confocal scanning microscopic images of a triangular prism crystal of ZJU-28 DPASD in a depth scanning mode imaged using SHG signals. c) Comparison of the SHG intensities of  $\alpha$  quartz, ZJU-28, and the chromophore-including ZJU-28.

from NLO inactive to NLO active materials ZJU-28 DPASB, ZJU-28 DPASN, and ZJU-28 DPASD observed at 532 nm, with powder SHG intensities of 0.25, 0.28, 3.5, and 18.3, respectively, versus  $\alpha$  quartz. The high SHG intensity of 18.3 in ZJU-28 DPASD is remarkable. The SHG intensity is proportional to the square of the energy of the fundamental frequency beam. In theory, the SHG intensity  $I_{2\omega}$  from any interface of the crystals in either reflection or transmission geometry is proportional to the square of the NLO coefficient  $\chi^{(2)}$  and to the energy of the fundamental frequency beam  $I_\omega$  [Eq. (1)]:

$$I_{2\omega} = \frac{32\pi^3 \omega^2 s^2 \theta_{2\omega}}{c^3} |e_{2\omega} \cdot \chi^{(2)} e_\omega|^2 I_\omega^2 \propto (\chi^{(2)})^2 I_\omega^2 \quad (1)$$

where  $\theta$  is the angle from the surface normal, at which the SHG signal occurs, the vectors  $e_\omega$  and  $e_{2\omega}$  describe the fundamental and the second harmonic light fields at the

surface.<sup>[30]</sup> Studies indicated that the measured SHG intensity of ZJU-28 DPASD matches with the theoretically calculated intensity, which indicates that the second-order nonlinear optical effect indeed occurs in ZJU-28 DPASD and is attributed to the acentric orientation of the chromophore DPASD ions in ZJU-28 DPASD.

Using the confocal laser scanning microscope equipped with a femtosecond laser pulsed at 1040 nm, the SHG response of ZJU-28 DPASD was imaged by collecting the SHG signal at 520 nm (Figure 3b). The slices of the SHG images in different depths display a uniform SHG distribution in the single crystal, further indicating that the NLO activity originates from the ordered chromophores in the host MOF ZJU-28.

Exact pore/channel matching with the included hemicyanine chromophores and strong interactions between the host framework and the included hemicyanine chromophore guest ions are important for stabilizing the highly ordered NLO active hemicyanine chromophore guest ions to generate nonlinear optical properties. As shown before, the SHG intensities of the examined materials are heavily dependent on the included hemicyanine chromophore guest ions: the longer the terminal alkyl chain of the included hemicyanine chromophore guest ions, the stronger the SHG intensity of the resulting MOF material. In fact, the SHG intensity of ZJU-28 DPASD is about 73 times higher than that of ZJU-28 DPASB. It is speculated that the longer alkyl chain minimizes the rotational freedom of the included hemicyanine chromophore guest ions and enhances the interactions with the host framework, leading to the most ordered DPASD ions in the 1D channels of the ZJU-28 framework. Given the fact that DPASD is a basically linear molecule, 1D pore channel confinement within porous MOF materials is necessary for the incorporation of the ordered dipolar chromophores and generation of second-order nonlinear optical activity. For comparison, a DPASD-including MOF NOTT-210 DPASD (NOTT-210 = In-TPTC, TPTC = terphenyl-3,3',5,5'-tetracarboxylic acid)<sup>[31]</sup> with 3D intersecting pores/channels of about  $6.1 \times 12.0$  and  $6.8 \times 6.8 \text{ \AA}^2$  has no detectable SHG signals. Furthermore, the MOF bio-MOF-1 DPASD (bio-MOF-1 =  $\text{Zn}_8(\text{ad})_4(\text{BPDC})_6\text{O} \cdot 2\text{Me}_2\text{NH}_2$ , ad = adeninate, BPDC = biphenyldicarboxylate),<sup>[32]</sup> with larger 1D pore channels of about  $5.8 \times 5.8$  and  $8.9 \times 8.9 \text{ \AA}^2$  does not show any NLO properties because of the poor pore channel confinement of bio-MOF-1 for the DPASD ions (Figure S9–S14).

Nonlinear optical MOF materials have been exclusively constructed from dipolar organic linkers before.<sup>[11]</sup> This traditional strategy still suffers from unpredictable resulting MOF structures which do not necessarily fulfill the requirement of noncentrosymmetric crystal packing. As shown in our first example of the anionic MOF ZJU-28 which was used to align ordered pyridinium hemicyanine chromophores into the 1D channels and generate high nonlinear optical activity, we developed an approach to construct NLO MOF materials. This strategy will broaden research on NLO MOF materials because any kind of organic linker can now be used. The combination of a wide variety of dipolar organic chromophores with high  $\beta$  values and MOF materials of diverse pore/



channel structures and tunable pore/channel sizes will result in highly active NLO MOF materials in the future.

## Experimental Section

Synthesis of  $[(\text{CH}_3)_2\text{NH}_2]_3[\text{In}_3(\text{BTB})_4] \cdot 12\text{DMF} \cdot 22\text{H}_2\text{O}$  (ZJU-28): In a solution of DMF (36 mL), 1,4-dioxane (24 mL), water (4 mL), and nitric acid (0.25 mL) 4,4',4''-benzene-1,3,5-triyl-tri-benzoic acid ( $\text{H}_3\text{BTB}$ , 532.0 mg, 1.2 mmol) and  $\text{InCl}_3$  (582.4 mg, 2.4 mmol) were dissolved. After the resulting solution had been kept at 130 °C for 24 h, it was cooled to room temperature and colorless needle-like crystals were collected by filtration and washed with DMF (0.81 g, 58 % based on  $\text{H}_3\text{BTB}$ ). Elemental analysis: Calcd (%) for  $[(\text{CH}_3)_2\text{NH}_2]_3[\text{In}_3(\text{BTB})_4] \cdot 12\text{DMF} \cdot 22\text{H}_2\text{O}$  ( $\text{C}_{150}\text{H}_{212}\text{In}_3\text{N}_{15}\text{O}_{58}$ , 3496.12): C, 51.51; H, 6.11; N, 6.01; Found: C, 51.14; H, 5.48; N, 6.65.

Single-crystal data were collected on an Oxford Xcalibur Gemini Ultra diffractometer with an Atlas detector. The data were collected using graphite monochromatic  $\text{Cu-K}_\alpha$  radiation ( $\lambda = 1.54178 \text{ \AA}$ ) at 293 K. The data sets were corrected by empirical absorption correction using spherical harmonics, implemented in the SCALE3 ABSPACK scaling algorithm. The structure was solved by direct methods, and refined by full-matrix least-square methods with the SHELX-97 program package. The hydrogen atoms were refined with geometric constraints. The solvents in the crystal are highly disordered, and the SQUEEZE subroutine of the PLATON software suit was conducted. X-ray crystal data for ZJU-28:  $\text{C}_{108}\text{H}_{60}\text{In}_3\text{O}_{24}$ ,  $M_w = 2086.02$ ,  $0.15 \times 0.23 \times 0.49 \text{ mm}^3$ , hexagonal,  $P6_3c$   $a = b = 26.4797(9) \text{ \AA}$ ,  $c = 17.4830(4) \text{ \AA}$ ,  $V = 10616.3(6) \text{ \AA}^3$ ,  $Z = 2$ ,  $T = 293 \text{ K}$ ,  $\rho_{\text{calcd}} = 0.653 \text{ g cm}^{-3}$ ,  $\mu = 2.864 \text{ mm}^{-1}$ ,  $F(000) = 2094$ , 50712 reflections, 6565 independent reflections,  $R_{\text{int}} = 0.122$ ,  $R_1[I > 2\sigma(I)] = 0.0712$ ,  $wR_2 = 0.1782$ , GOF = 1.057. CCDC 884010 contains the supplementary crystallographic data for this paper. These data can be obtained free of charge from The Cambridge Crystallographic Data Centre via [www.ccdc.cam.ac.uk/data\\_request/cif](http://www.ccdc.cam.ac.uk/data_request/cif).

Received: May 29, 2012

Published online: July 18, 2012

**Keywords:** chromophores · ion exchange · mesoporous materials · metal–organic frameworks · nonlinear optics

- [1] L. R. Dalton, P. A. Sullivan, D. H. Bale, *Chem. Rev.* **2010**, *110*, 25–55.
- [2] T. P. Radhakrishnan, *Acc. Chem. Res.* **2008**, *41*, 367–376.
- [3] D. Frattarelli, M. Schiavo, A. Facchetti, M. A. Ratner, T. J. Marks, *J. Am. Chem. Soc.* **2009**, *131*, 12595–12612.
- [4] Z. Li, W. Wu, Q. Li, G. Yu, L. Xiao, Y. Liu, C. Ye, J. Qin, Z. Li, *Angew. Chem.* **2010**, *122*, 2823–2827; *Angew. Chem. Int. Ed.* **2010**, *49*, 2763–2767.
- [5] Y. Liao, S. Bhattacharjee, K. A. Firestone, B. E. Eichinger, R. Paranj, C. A. Anderson, B. H. Robinson, P. J. Reid, L. R. Dalton, *J. Am. Chem. Soc.* **2006**, *128*, 6847–6853.
- [6] J. Gao, Y. Cui, J. Yu, Z. Wang, M. Wang, J. Qiu, G. Qian, *Macromolecules* **2009**, *42*, 2198–2203.
- [7] W. Lin, Y. Cui, J. Gao, J. Yu, T. Liang, G. Qian, *J. Mater. Chem.* **2012**, *22*, 9202–9208.
- [8] M. O’Keeffe, O. M. Yaghi, *Chem. Rev.* **2012**, *112*, 675–702.
- [9] B. Chen, S. Xiang, G. Qian, *Acc. Chem. Res.* **2010**, *43*, 1115–1124.
- [10] Y. Cui, Y. Yue, G. Qian, B. Chen, *Chem. Rev.* **2012**, *112*, 1126–1162.
- [11] C. Wang, T. Zhang, W. Lin, *Chem. Rev.* **2012**, *112*, 1084–1104.
- [12] J. P. Zhang, Y. B. Zhang, J. B. Lin, X. M. Chen, *Chem. Rev.* **2012**, *112*, 1001–1033.
- [13] G. K. H. Shimizu, R. Vaidhyanathan, J. M. Taylor, *Chem. Soc. Rev.* **2009**, *38*, 1430–1449.
- [14] J. R. Li, J. Sculley, H. C. Zhou, *Chem. Rev.* **2012**, *112*, 869–932.
- [15] H.-L. Jiang, Y. Tatsu, Z.-H. Lu, Q. Xu, *J. Am. Chem. Soc.* **2010**, *132*, 5586–5587.
- [16] S.-T. Zheng, J. J. Bu, T. Wu, C. Chou, P. Feng, X. Bu, *Angew. Chem.* **2011**, *123*, 9020–9024; *Angew. Chem. Int. Ed.* **2011**, *50*, 8858–8862.
- [17] Y. Liu, X. Xu, F. Zheng, Y. Cui, *Angew. Chem.* **2008**, *120*, 4614–4617; *Angew. Chem. Int. Ed.* **2008**, *47*, 4538–4541.
- [18] Y. Liu, G. Li, X. Li, Y. Cui, *Angew. Chem.* **2007**, *119*, 6417–6420; *Angew. Chem. Int. Ed.* **2007**, *46*, 6301–6304.
- [19] J. An, C. M. Shade, D. A. Chengelis-Czegan, S. P. Petoud, N. L. Rosi, *J. Am. Chem. Soc.* **2011**, *133*, 1220–1223.
- [20] C. Wang, K. E. deKrafft, W. Lin, *J. Am. Chem. Soc.* **2012**, *134*, 7211–7214.
- [21] W. Zhou, H. Wu, T. Yildirim, *J. Am. Chem. Soc.* **2008**, *130*, 15268–15269.
- [22] S. Yang, X. Lin, A. J. Blake, G. S. Walker, P. Hubberstey, N. R. Champness, M. Schröder, *Nat. Chem.* **2009**, *1*, 487–493.
- [23] S. Yang, X. Lin, W. Lewis, M. Suyetin, E. Bichoutskaia, J. E. Parker, C. C. Tang, D. R. Allan, P. J. Rizkallah, P. Hubberstey, N. R. Champness, K. Mark Thomas, A. J. Blake, M. Schröder, *Nat. Mater.* **2012**, DOI: 10.1038/nmat3343.
- [24] T. Uemura, D. Hiramatsu, Y. Kubota, M. Takata, S. Kitagawa, *Angew. Chem.* **2007**, *119*, 5075–5078; *Angew. Chem. Int. Ed.* **2007**, *46*, 4987–4990.
- [25] T. Uemura, N. Yanai, S. Kitagawa, *Chem. Soc. Rev.* **2009**, *38*, 1228–1236.
- [26] L. Alaerts, C. E. A. Kirschhock, M. Maes, M. A. van der Veen, V. Finsy, A. Depla, J. A. Martens, G. V. Baron, P. A. Jacobs, J. E. M. Denayer, D. E. De Vos, *Angew. Chem.* **2007**, *119*, 4371–4375; *Angew. Chem. Int. Ed.* **2007**, *46*, 4293–4297.
- [27] O. Delgado-Friedrichs, M. O’Keeffe, O. M. Yaghi, *Phys. Chem. Chem. Phys.* **2007**, *9*, 1035–1043.
- [28] M. O’Keeffe, M. A. Peskov, S. J. Ramsden, O. M. Yaghi, *Acc. Chem. Res.* **2008**, *41*, 1782–1789.
- [29] S. K. Kurtz, T. T. Perry, *J. Appl. Phys.* **1968**, *39*, 3798–3813.
- [30] R. M. Corn, D. A. Higgins, *Chem. Rev.* **1994**, *94*, 107–125.
- [31] S. Yang, S. K. Callear, A. J. Ramirez-Cuesta, W. I. F. David, J. Sun, A. J. Blake, N. R. Champness, M. Schröder, *Faraday Discuss.* **2011**, *151*, 19–36.
- [32] J. An, N. L. Rosi, *J. Am. Chem. Soc.* **2010**, *132*, 5578–5579.